

## PECULIARITIES OF FLASH-BUTT WELDING OF RAIL FROGS WITH RAIL ENDS

A.V. KAVUNICHENKO, V.I. SHVETS and E.V. ANTIPIN

E.O. Paton Electric Welding Institute of the NAS of Ukraine  
11 Kazimir Malevich Str., 03150, Kyiv, Ukraine. E-mail: [office@paton.kiev.ua](mailto:office@paton.kiev.ua)

Producing of quality welded joints of rail frogs of steel 110G13L with rail ends without an intermediate insert is still an urgent problem. The results of investigations of formation of welded joints of rail steel M76 with steel 110G13L made by the flash-butt welding without an austenitic insert. are presented. It was shown that in the near-contact layer of rail steel, the high-alloy unstable austenite, fringed with carbides, is formed. It was established that localization of internal stresses and the presence of embrittling structures are the cause of a low deflection at the required fracture force of welded joints. 7 Ref., 2 Tables, 9 Figures.

**Keywords:** flash-butt welding, steel 110G13L, rail steel M76, microstructure, heat treatment, nonmetallic inclusions, internal stresses, mechanical properties, carbides, unstable austenite

At the enterprises of the railways of Ukraine, a large number of railway frogs are used, which are joined with a rail by bolts.

At the E.O. Paton Electric Welding Institute the technology of flash-butt welding of railway frogs, made of steel 110G13L with rail ends (steel M76) through an intermediate insert was developed using a pulse flashing [1]. The developed technology envisages the use of an intermediate austenitic insert of a standard production in the joints without a subsequent heat treatment [2].

At the same time, the attempts are still made to produce a quality joint of railway frogs from 110G13L steel with rail ends directly (without an intermediate insert).

The aim of this work is to investigate the peculiar features of formation and properties of joints of rail steel with steel 110G13L without an intermediate insert by using the flash-butt welding (FBW).

The welding of a pilot batch was carried out on castings of steel 110G13L in the form of a rail profile R65 and rail steel (Table 1) using the technology developed at the E.O. Paton Electric Welding Institute [3]. The parameters of the welding process varied in wide ranges:

- duration of welding process is 60–120 s;
- allowance for welding is  $24 \pm 1$ – $30 \pm 1$  mm;
- final speed of forcing is 1.0–1.4 mm/s;

- upsetting value is 10–14 mm.

The metallographic examinations and analysis of chemical heterogeneity of joints metal were carried out in the optical microscope «Neophot-32» and in the microanalyzer SX-50 of the «Camebax» Company.

The carried out examinations showed that microstructures of the joints of rail steel with steel 110G13L have a similar nature. Therefore, for discussion, the joint was selected, produced at the following mode:

- duration of welding process is 75 s;
- allowance for welding is  $26 \pm 1$  mm;
- final speed of forcing is 1.2 mm/s;
- upsetting value is 12 mm.

During analysis of the microstructure the following sections of a joint were selected for discussion: HAZ of rail steel, HAZ of steel 110G13L, transition zone at the contact boundary.

In the HAZ metal of rail steel (similar to the homogeneous joint), the microstructure of hardening sorbite is preserved. The effect of welding heat is pronounced by an increase in size of primary austenite grains at approaching the joint line.

In contrast to rail steel, the steel 110G13L is thermally unstable [4].

In the temperature range of 400–700 °C, already at the short-time heating, a decay of austenite by the reaction  $\gamma \rightarrow \gamma_{\text{depl}} + (\text{Fe, Mn})_3\text{C}$  is possible. In its turn, the austenite, depleted with carbon and manganese,

**Table 1.** Chemical composition of steels (wt.%) and their melting range

Steel	Mn	Si	C	P	S	Cu	$T_{\text{sol}} - T_{\text{liq}}, ^\circ\text{C}$
M76	0.81	0.029	0.724	0.007	0.014	–	1380–1470
110G13L	14.1	–	1.2	0.03	0.002	–	1330–1375

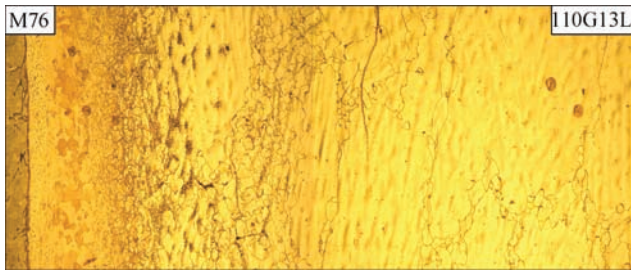


**Figure 1.** Microstructure ( $\times 50$ ) of joint of steel 110G13L with steel M76

can further decay with the formation of troostite-sorbite structures [5].

In the joint, the precipitation of carbides is observed in the region at a distance of about 1 mm from the joint (Figure 1). The carbides are precipitated along the grain boundaries. In the middle part of the marked section, the development of the process leads to the formation of a solid carbide network (Figure 2, *b*). The appearance of acicular carbides of crystallographic orientation, growing from the boundary, is possible. It should be noted that in the area of carbides region the fine globular formations are observed, the nature of which requires additional investigations.

The austenite layer of a polyhedral structure, which is formed under the conditions of homogenization annealing, is adjacent to the joint line. In the near-contact zone, a partial melting of grain sub-boundaries is possible in this layer (Figure 2, *a*).

The formation of the transition zone at the contact boundary with rail steel occurs as a result of solid-liquid interaction with the melt of steel 110G13L, the melting interval of which is significantly lower (see Table 1).

During analysis of microstructure of the transition zone, it was established that in rail steel at a depth of 2–3 mm from the joint line between the blocks of grains (Figure 3) a structural component of light color is formed (conventionally called the interblock structure — ISC).

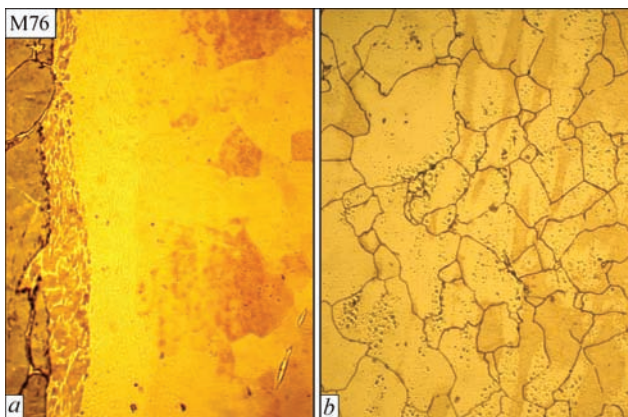


**Figure 2.** Microstructure ( $\times 200$ ) of the characteristic sections of the HAZ metal of steel 110G13L: *a* — near-contact layer with partial melting of grain sub-boundaries; *b* — carbide network along the grain boundaries

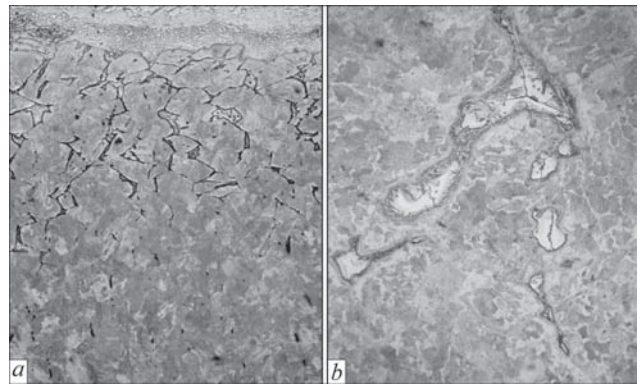


**Figure 3.** ISC in rail steel M76: *a* —  $\times 50$ ; *b* —  $\times 400$

Within the ISC, the presence of nonmetallic inclusions, eutectic colonies, is possible.

According to the results of the X-ray spectral microanalysis, the base of ISC consists of iron, containing in wt.%: 4–8 Mn and 0.9–2.4 C. The microhardness of ISC of about  $HV\ 0.2\text{--}2570$  corresponds to the microhardness of high-alloy unstable austenite. The trend of the carbon distribution curve gives assumption that the ISC is fringed with carbides, presumably  $(Fe, Mn)_3C$  (Figure 4).

It is supposed that the formation of ISC occurs at the first stage of concentration melting of metal around the nonmetallic inclusions, located mainly along the grain boundaries (in the systems Fe–Mn–S, Fe–P, Fe–Mn–P, Fe–Cr–Ni–Ti–C there are eutectics with  $T_e$  about  $1000\text{ }^\circ\text{C}$ ). Then the processes of diffusion transfer to the melt of the base metal elements with higher solubility in the liquid phase (carbon, manganese) and mass transfer of the melt from the boundary along the fused grains follow.

In the joint transition zone a layer is adjoined to rail steel, which includes the dark color formation of

**Chemical composition of microvolumes of ISC, wt.%**  
(see Figure 4)

No.	Si	Cr	Ti	Ni	Fe	Mn	C
1	0.486	0.095	0.000	0.004	92.882	4.088	2.438
2	0.589	0.096	0.006	0.000	92.998	4.382	1.979
3	0.512	0.080	0.026	0.014	93.768	3.813	1.736
4	0.473	0.142	0.058	0.004	89.686	8.721	0.911

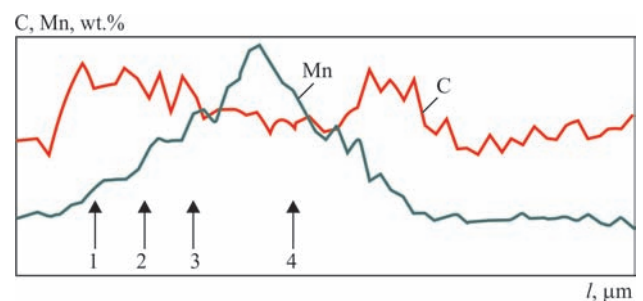


**Figure 4.** Distribution of carbon and manganese in ISC. Results of analysis of chemical composition of metal microvolumes within ISC



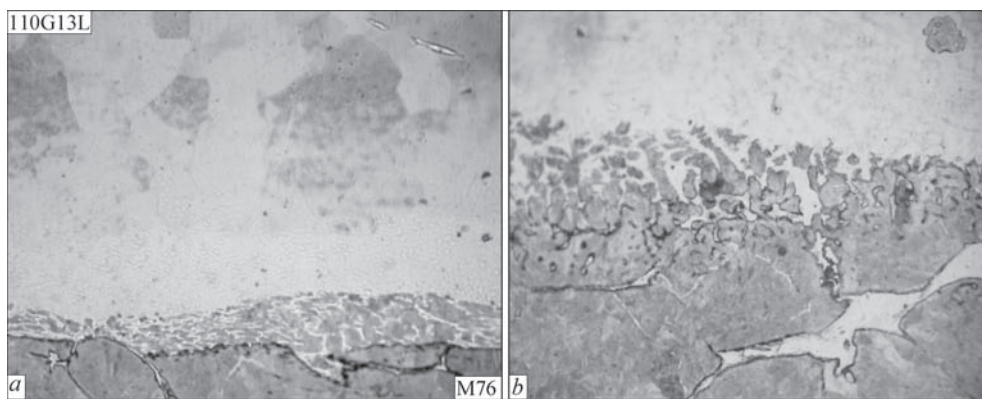


**Figure 5.** Microstructure of transition zone at the contact boundary of rail steel M76 and Hadfield steel: *a* —  $\times 200$ ; *b* —  $\times 400$

irregular shape, which in some cases is acicular. The appearance of this layer is not regular (Figure 5).

According to the results of X-ray spectral microanalysis (Figure 6), the concentration of manganese and carbon varies stepwise in the region of the transition zone without the layer. The width of diffusion zones in both steels amounted to about 5  $\mu\text{m}$  (Figure 6, *b*).

In the region with the layer, on the curve of manganese distribution a step of about 65  $\mu\text{m}$  width (Figure 6, *a*) with an intermediate value of manganese concentration of 3.5–4.5 wt.% is observed. The con-

centration of carbon in this case is at the level of that of steel 110G13L.

Obviously, the layer was formed as a result of partial dissolution of rail steel and the subsequent crystallization of excessive phases on residual particles. In the case when the melt with particles is almost completely squeezed out during upsetting (or only the frontal dissolution of rail steel takes place), the layer is absent. In this case the joint is formed similarly to the joints produced during solid-phase interaction.

The strength characteristics of such a welded joint are low. The fracture occurs in the near-contact layer of rail steel at a distance of up to 2 mm from the joint line. The ISC inclusions, fringed by carbides, as well as boundaries of grain blocks with carbide precipitations are critical for the strength under the conditions of high postweld stresses due to a large difference in the coefficient of thermal expansion (CTE) of steels being joined.

The ability of transformation of non-desirable structural components with the use of heat treatment was considered. The effect of annealing was studied at the following modes:

1.  $T = 350\text{ }^\circ\text{C}$ , 3 h, oil cooling (tempering);
2.  $T = 850\text{ }^\circ\text{C}$ , 3 h, oil cooling (normalization);

**Chemical composition of layer microvolumes having fragments with the hardening structure of iron-carbon steels, wt.%**

No.	Si	Cr	Ti	Ni	Fe	Mn	C
1	0.453	0.056	0.025	0.000	94.882	3.877	0.707
2	0.553	0.063	0.028	0.042	94.996	4.123	0.796
3	0.445	0.062	0.027	0.007	94.275	4.879	0.620
4	0.456	0.046	0.016	0.028	90.301	4.433	4.664

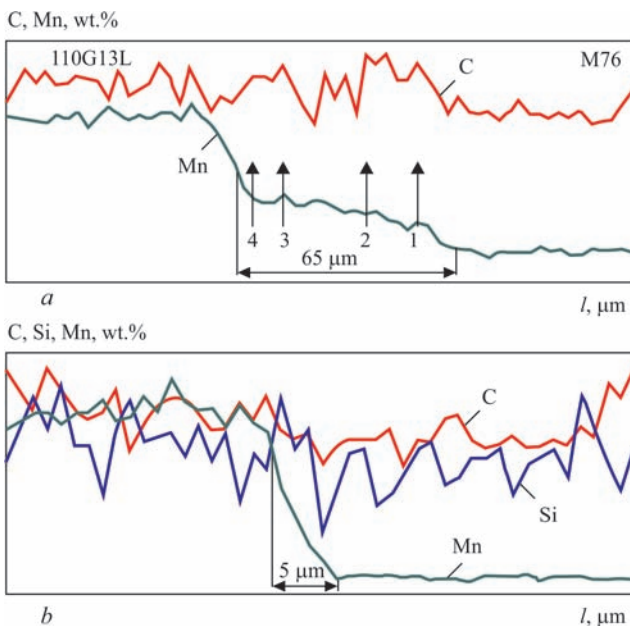


**Figure 6.** Distribution of elements in the transition zone of a joint of rail steel M76 and Hadfield steel in the region: *a* — with acicular phase; *b* — without acicular phase

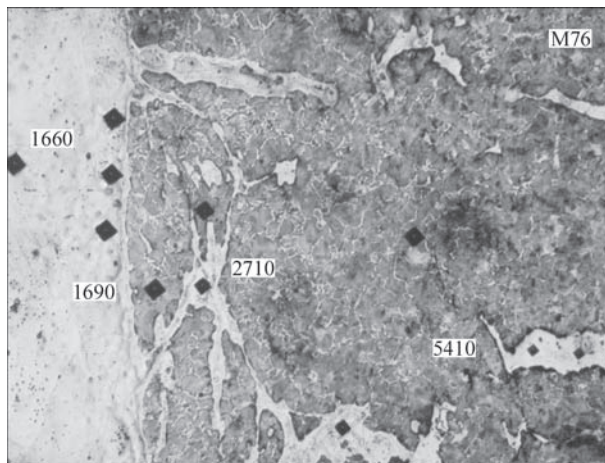


**Figure 7.** Microstructure ( $\times 400$ ) and distribution of microhardness in the joint of rail steel M76 and Hadfield steel after annealing by the mode:  $T = 850\text{ }^\circ\text{C}$ ,  $\tau = 3\text{ h}$ , oil cooling

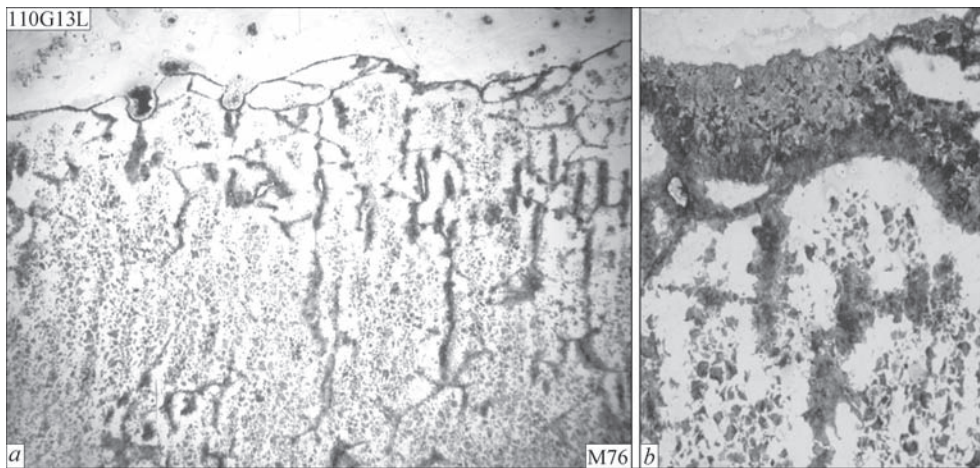


**Figure 8.** Microstructure of welded joint of rail steel with steel 110G13L after annealing by the mode 3: *a* —  $\times 50$ ; *b* —  $\times 400$

3.  $T = 1000$  °C, 3 h, oil cooling (homogenizing annealing).

Annealing by the mode 1 affects the change in the hardness of structural components. The hardness of ISC ( $HV$  0.5–3810) and the hardness in the areas with dark formations in the layer along rail steel ( $HV$  0.5–5430) is increased. The microhardness of steel 110G13L and rail steel properly in the near-contact zone decreased and amounted to  $HV$  0.5–1600–2000 and  $HV$  0.5–1800–2000, respectively.

After recrystallization by the mode 2, the dark formations in the layer along the contact boundary of rail steel as well as the fringing of carbides at the ISC boundary with the base metal, disappear in the microstructure of the transition zone. In this case, the hardness of ISC increases to  $HV$  0.5–5500 (Figure 7). Apparently, on the one hand, the observed changes are caused by the dissolution of carbides in the austenite matrix at the temperatures higher than  $A_3$  point, and on the other hand, by the formation of martensite in the metastable austenite of ISC. The microstructure of rail steel in the near-contact zone represents refined pearlite colonies with a ferrite fringing and microhardness of  $HV$  0.5–1830, which is lower than that at a distance of 4 mm from the contact boundary  $HV$  0.5–2600. The values of microhardness in the near-contact zone of Hadfield steel are in the range of  $HV$  0.5–1600–1750.

The results of homogenizing annealing of the joint by the mode 3 are of interest. As is seen (Figure 8), after heat treatment, ISC are completely or partially transformed into pearlite with microhardness of  $HV$  0.5–1850–2310. The observed residual regions of ISC, surrounded by pearlite, preserve the microhardness of high-alloy austenite of  $HV$  0.5–3220–4390.

It should be noted that microhardness of austenitic grains of steel 110G13L after homogenizing annealing remains at the same level ( $HV$  0.5–2440–3200)

with a significant reduction in the microhardness of rail steel ( $HV$  0.5–1190).

The homogenizing annealing appears to be promising for eliminating undesired structural components formed in rail steel. However, the capabilities of post-weld heat treatment are limited by carbide formation in steel 110G13L, occurring in the temperature range of 250–950 °C. To preserve the properties of steel 110G13L, the quenching from the homogenizing temperatures is required. This may cause the formation of martensite in rail steel, which, in its turn, is unacceptable.

In connection with the fact that the fracture of welded joints during tests on static bending occurs at relatively small deflection, the investigations were carried out to determine residual stresses in welded joints which can reduce the deformability, as well as the fatigue strength of the welded joint. To calculate

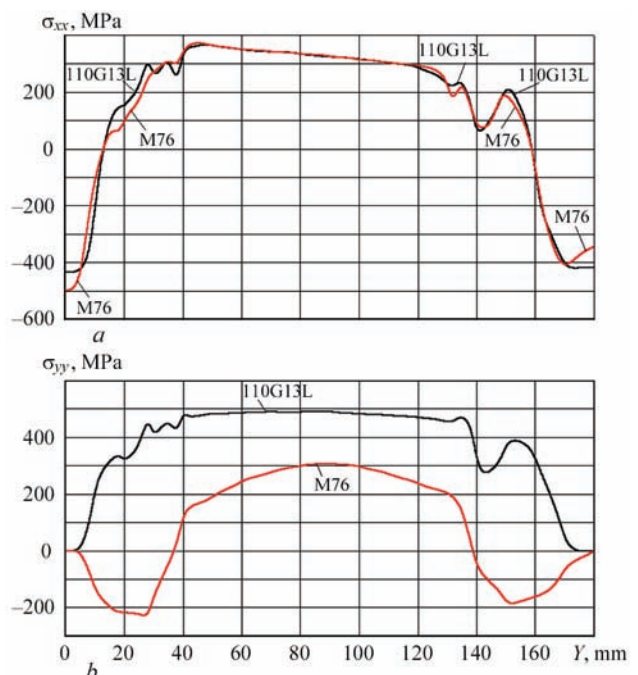


**Figure 9.** Distribution of residual stresses  $\sigma_{xx}$  (*a*) and  $\sigma_{yy}$  (*b*) along the joint at a distance  $x = 2.5$  mm (M76) and  $x = -2.5$  mm (110G13L)

**Table 2.** Results of tests of welded specimens on static bending (R65 profile)

No. of specimen	Fracture force, kN	Deflection, mm
1	1000	12
2	900	13
3	980	17
4	1050	19
5	1000	19
6	800	11
7	1000	12
8	1100	15
9	1100	13
10	900	12
11	1150	17

the stressed state, an algorithm for numerical solution of the problem of non-isothermal plastic flow with the Mises yield criterion was used.

The analysis of the calculation data of residual stresses, presented in Figure 9 for joints of steel 110G13L with rail steel showed that the beginning of crack formation in the transition zone of a joint in the web of the rail profile is determined by the presence of tensile residual stresses  $\sigma_{xx}$ , the values of which are the highest ones in the wall near the transition to the flange.

The use of welding modes with increased specific powers led to decrease in the level of residual stresses in welded joint, which made it possible to produce full-profile welded joints which did not fracture spontaneously. The testing of welded joints of full-profile specimens on static transverse bending at a certain destructive force did not demonstrate stable results by deflection (the deflection is in the range of 8–19 mm, see Table 2), which does not meet the requirements of the Ukrainian and European standards [6, 7].

## Conclusions

1. In the transition zone of the joint of steel 110G13L with rail steel, produced by FBW, the structural components of the intermediate chemical composition are formed.

2. In the near-contact layer of rail steel, the so-called interblock structural component (ISC) is formed, representing a high-alloy unstable austenite, fringed by carbides.

3. In the transition zone along the boundary of rail steel, the layers with products of dissolution of rail steel and the subsequent crystallization of carbides on them are formed.

4. The formation of cracks in the fusion zone along the joint can be related to the presence of residual tensile stresses  $\sigma_{xx}$  whose values are the highest ones in the wall near the transition to the flange.

5. The localization of internal stresses in the weld due to a large difference in CTE of the steels joined (almost 2 times) and the presence of embrittling structural components are the cause of the joint low strength.

6. The use of postweld heat treatment is problematic as far as there is no coincidence between the permissible modes of heat treatment for rail steel and steel 110G13L.

7. The technological measures preventing the formation of the mentioned defects should be aimed at increasing the resistance of the fusion zone material to occurrence of the corresponding cracks; from these positions, the use of an intermediate austenitic insert containing nickel is one of the effective technological means in this direction.

1. Kuchuk-Yatsenko, S.I., Shvets, V.I., Gordan, G.N. et al. (2006) Features of formation of structure of joints of rail steel M76 to steel 110G13L made by flash-butt welding. *The Paton Welding J.*, **1**, 2–8.
2. Kuchuk-Yatsenko, S.I., Shvets, Yu.V., Dumchev, E.A. et al. (2005) Flash-butt welding of railway frogs with rail ends using an intermediate insert. *Ibid.*, **1**, 2–4.
3. Kuchuk-Yatsenko, S.I., Didkovsky, O.V., Bogorsky, M.V. et al. (2002) *Method of flash-butt welding*. Ukraine, Pat. 46820. Int. Cl. B23K 11/04 [in Ukrainian].
4. Gruzin, P.L., Grigorkin, V.I., Moskaleva, L.N., Mural, V.V. (1969) Transformations in austenitic manganese steel. *Metall-ovedenie i Termich. Obrab. Metallov*, **1**, 5–9 [in Russian].
5. Tkachenko, F.K., Efremenko, V.G. (1990) Structure and phase transformations in wrought high-manganese steel. *Ibid.*, **2**, 8–10 [in Russian].
6. (2006) *TU U 27.3-26524137-1342:2006*: Frogs and cores with welded-up rail ends of R65, R50 and UIC60 types. Specification [in Ukrainian].
7. (2012) *DIN EN 14587-3:2012*: Railway applications — Track-flash butt welding of rails. Pt 3: Welding in association with crossing construction.

Received 14.03.2018